Enhancing chaoticity of spatiotemporal chaos

Xiaowen Li,[1] Heqiao Zhang,[1] Yu Xue,[1,2] and Gang Hu[3,1,4,*]
[1]*Department of Physics, Beijing Normal University, Beijing 100875, People's Republic of China*
[2]*Department of Physics, Guangxi University, Nanning 530003, People's Republic of China*
[3]*China Center for Advanced Science and Technology (CCAST) (World Laboratory), P.O. Box 8730, Beijing 100080, People's Republic of China*
[4]*The Key Laboratory of Beam Technology and Material Modification of the Ministry of Education, Beijing Normal University, Beijing 100875, People's Republic of China*
(Received 1 June 2004; revised manuscript received 29 October 2004; published 14 January 2005)

In some practical situations strong chaos is needed. This introduces the task of chaos control with enhancing chaoticity rather than suppressing chaoticity. In this paper a simple method of linear amplifications incorporating modulo operations is suggested to make spatiotemporal systems, which may be originally chaotic or nonchaotic, strongly chaotic. Specifically, this control can eliminate periodic windows, increase the values and the number of positive Lyapunov exponents, make the probability distributions of the output chaotic sequences more homogeneous, and reduce the correlations of chaotic outputs for different times and different space units. The applicability of the method to practical tasks, in particular to random number generators and secure communications, is briefly discussed.

DOI: 10.1103/PhysRevE.71.016216 PACS number(s): 05.45.Xt, 05.45.Jn

I. INTRODUCTION

Since the pioneering work of Ott, Grebogi, and Yorke (OGY) [1], the topic of chaos control has attracted much attention in the nonlinear science community as well as in diverse related fields [2–8]. Most works on chaos control have been focused on the suppression of chaotic motion. However, suppressing (or killing) chaos is not the only interest of chaos control. In some realistic applications chaoticity is a desirable property, which should be developed and used (one of the typical examples is chaos communication). Recently a few works have studied the problem of how to make dynamical systems chaotic. This includes how to make nonchaotic systems chaotic and how to change less chaotic systems to be more intensively chaotic [9–18]. Nevertheless, there are still very few systematic investigations in this direction.

In this paper it is our task to suggest a systematic as well as simple scheme to modify nonlinear systems (which may be chaotic or nonchaotic originally) to be excellently chaotic (the meaning of "excellently chaotic" will be explained later). Since spatiotemporal chaos is expected to have, in many realistic situations, much more useful applications than low-dimensional chaos, we will consider coupled chaotic maps as our model. In Sec. II, this model system will be introduced, and a number of disadvantages of the system about its chaoticity will be discussed. In Sec. III, we will modify the coupled chaotic map lattice by combining linear amplifications and modulo operations. With these simple changes, the modified spatiotemporal system has excellent chaotic properties, such as the absence of periodic windows, larger values and larger number of positive Lyapunov exponents, homogeneous probability distribution of chaotic sequences, extremely short correlation time, and short spatial correlation distance of various chaotic sequences. In Sec. IV, possible applications of this scheme to random number generators and secure communications are briefly discussed. The extension of this method to different spatiotemporal chaotic systems is also emphasized in this section.

II. MODEL

We consider the following one-way ring of coupled map lattice (CML):

$$x_{n+1}(i) = (1-\varepsilon) f(x_n(i)) + \varepsilon f(x_n(i-1)), \tag{1a}$$

$$i = 1,2,\ldots,N, \quad x_n(i+N) = x_n(i). \tag{1b}$$

For the local dynamics, we use the logistic map with fully developed chaos,

$$f(x) = 4x(1-x). \tag{2}$$

In Eq. (1) we use the coupling ε as the adjustable parameter. As $\varepsilon=0$ or $\varepsilon=1$, we recover the results of a single logistic map. For $0<\varepsilon<1$, the coupling plays an essential role in changing the dynamic behavior of the system. Let us first study the features of Eq. (1). Without losing generality we fix the system size $N=10$. Extensions to the cases of general system sizes will be discussed in Sec. IV. Though there have been many works investigating system (1) [19–23], some features of Eq. (1) still have not been completely revealed. In the following we will show some characteristic behaviors of Eq. (1).

The following dynamical properties of the CML system are of great interest and significance: (i) the chaotic and periodic parameter regions; (ii) the largest Lyapunov exponent and the numbers of positive Lyapunov exponents; (iii) the probability distributions of chaotic sequences for different

*Corresponding author.

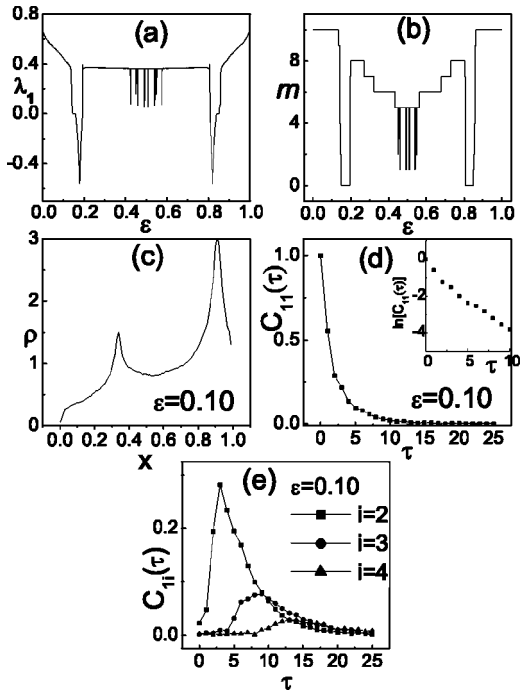

FIG. 1. Numerical results of the CML system Eq. (1) with map function Eq. (2); $N=10$. (a) The largest Lyapunov exponent λ_1 vs coupling parameter ε. Nonchaotic windows have a finite measure in the parameter space. (b) The number of positive Lyapunov exponents m plotted vs ε. The regions where $m=N=10$ are very small, located near $\varepsilon=0$ and $\varepsilon=1$. (c), (d), (e) $\varepsilon=0.10$, corresponding to $\lambda_1=0.4518$ and $m=10$ for Eq. (1). (c) Probability distribution $\rho(x(1))$ plotted vs $x(1)$. 100 meshes and $M=10^6$ iterations are used for producing the distribution. The density of a given mesh x is computed as $\rho(x)=100(M_x/M)$ with M_x being the number of data falling in the mesh x. The distribution is strongly inhomogeneous. (d) Autocorrelation $C_{11}(\tau)$, defined in Eqs. (3) and (4), plotted vs τ. Nonzero $C_{11}(\tau)$ can be clearly seen for rather large τ (e.g., $\tau\leqslant 13$). (e) Mutual correlations [defined in Eq. (5)] $C_{12}(\tau)$, $C_{13}(\tau)$, and $C_{14}(\tau)$ plotted vs τ. Even between the first and the fouth sites, $C_{14}(\tau)$ is observably nonzero for $\tau<25$.

couplings; (iv) the temporal and spatial correlations of the output chaotic sequences. All these properties are crucial for applications of chaos, especially for the applications of chaos communications.

In Fig. 1(a) we plot the largest Lyapunov exponent λ_1 of the system against the coupling strength ε. λ_1 is positive in some regions, corresponding to chaotic motions. However, there exist some periodic and other nonchaotic windows, where $\lambda_1\leqslant 0$. The existence of these nonchaotic windows may be seriously harmful in applications, where any nonchaotic behavior should be avoided.

In Fig. 1(b) we plot the number of positive Lyapunov exponents m vs the coupling ε. $m=10$ is observed only in very small parameter regions near $\varepsilon=0$ and $\varepsilon=1$. We find $m<10$ in a large ε regions ($0.865>\varepsilon>0.135$) and $m=0$ in some ε areas of period windows. Though the local dynamics of Eq. (2) is fully developed chaos, the collective motion of the coupled spatiotemporal system can be nonchaotic or weakly chaotic in the sense that m is considerably smaller than the dimension of the system ($N=10$). These weakly chaotic motions are not good for chaos applications.

In Fig. 1(c) we measure the probability distribution of an output sequence from a site arbitrarily chosen for $\varepsilon=0.10$ at which the system possesses relatively strong chaos, i.e., the system has large λ_1 ($\lambda_1=0.452$) and large m ($m=10$). We find that even for this high-dimensional spatiotemporal chaos the probability distribution is still strongly inhomogeneous. The inhomogeneity exposes much information of the deterministic dynamics and this is a serious drawback when the random behavior of chaos is required. Figure 1(c) shows that the chaotic sequence may not meet the requirement of randomness even in the case of strongly chaotic motion of spatiotemporal chaos.

In Figs. 1(d) and 1(e) we compute various correlation functions. In Fig. 1(d) the autocorrelation $C_{11}(\tau)$, which is defined as

$$C_{ii}(\tau)=\hat{C}_{ii}(\tau)/\hat{C}_{ii}(0), \tag{3}$$

$$\hat{C}_{ii}(\tau)=\lim_{T\to\infty}\frac{1}{T}\sum_{n=1}^{T}x_n(i)x_{n+\tau}(i)-\left(\lim_{T\to\infty}\frac{1}{T}\sum_{n=1}^{T}x_n(i)\right)^2, \tag{4}$$

is plotted vs τ at $\varepsilon=0.10$. Nonzero autocorrelation can be clearly observed for even very large τ (e.g., for $\tau\leqslant 13$). Such long-term correlation is definitely harmful when one uses chaotic systems as random number generators. In Fig. 1(e), the mutual correlations $C_{12}(\tau)$, $C_{13}(\tau)$, and $C_{14}(\tau)$, which are defined as

$$C_{ij}(\tau)=\hat{C}_{ij}(\tau)/\sqrt{\hat{C}_{ii}(0)\hat{C}_{jj}(0)},$$

$$\hat{C}_{ij}(\tau)=\lim_{T\to\infty}\frac{1}{T}\sum_{n=1}^{T}x_n(i)x_{n+\tau}(j)-\left(\lim_{T\to\infty}\frac{1}{T}\sum_{n=1}^{T}x_n(i)\right)\times\left(\lim_{T\to\infty}\frac{1}{T}\sum_{n=1}^{T}x_n(j)\right), \tag{5}$$

are plotted against τ. Though the mutual correlation between two sites decreases as their space distance increases, this decreasing tendency is not fast so that the chaotic sequences of two nonadjacent sites still have observable nonzero mutual correlation. When we intend to output the chaotic sequences from different sites in parallel, these nonzero mutual correlations are often inadequate.

From Figs. 1(a)–1(e) we find that even for strongly chaotic and high-dimensional systems, there may still exist some serious disadvantages of chaoticity. It is the task of the next section to find simple methods to enhance the chaoticity of the system, i.e., one may introduce some modifications that can be easily realized to overcome all the drawbacks of Fig. 1, and make the system achieve the desirable chaoticity.

III. ENHANCING CHAOTICITY OF SPATIOTEMPORAL CHAOS

In order to improve the chaoticity properties of the CML system, we modify Eq. (1) by the following linear amplifications and modulo operations:

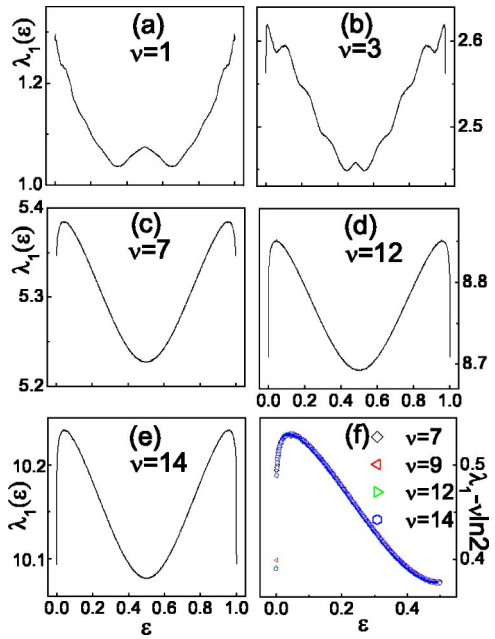

FIG. 2. (a)–(e) The same as Fig. 1(a) by computing Eq. (6) for different ν's. Nonchaotic windows disappear for $\nu \geqslant 1$. (f) As ν increases the function $\lambda(\varepsilon,\nu)-\nu \ln 2$ becomes independent of ν.

$$\hat{x}_{n+1}(i) = (1-\varepsilon) f(x_n(i)) + \varepsilon f(x_n(i-1)), \tag{6a}$$

$$x_{n+1}(i) = [2^{\nu} \hat{x}_{n+1}(i)] \bmod 1. \tag{6b}$$

We would like to emphasize that the control modifications Eq. (6) are simple and realizable in some practical applications. First, in computer simulations, the operation of Eq. (6b) does not cause any computational problem. Therefore the algorithm Eq. (6) can be directly used in practical applications of chaos communications with software realization. Second, for practical physical systems, there are many easy ways in realizing the linear-amplification operation [the multiple factor 2^{ν} in Eq. (6b)]. Moreover, by combining the results of comparisons and subtractions the modulo operations can be realized in electrical circuits without great difficulty. In Eq. (6b), the modulo is performed in the interval [0,1]. The features shown in Secs. III and IV do not change if the modulo interval is changed.

Some effects of Eq. (6b) can be intuitively estimated. For instance, increasing the linear multiple factor 2^{ν} will definitely increase the largest Lyapunov exponent of system Eq. (6). This makes the nonchaotic system chaotic, and makes chaos stronger. However, in order to fully understand the essential influences of operations Eq. (6b), and to explain how these control modifications can overcome the disadvantages of Eq. (1) shown in Figs. 1(a)–1(e), we should investigate Eq. (6) in detail.

First, we study how the modifications of Eq. (6b) can change the largest Lyapunov exponent and the period-window stucture. In Figs. 2(a)–2(e) we plot λ_1 of Eq. (6) vs ε for different ν's. We find that for $\nu \geqslant 1$, the nonchaotic windows of Fig. 1(a) disappear. It is interesting as well as surprising that as ν increases the function of $\lambda_1(\varepsilon,\nu)$ approaches a unique asymptotic form, which is independent of ν. $\lambda_1(\varepsilon,\nu)$ depends only on the dynamics of Eq. (6a). The unique asymptotic function can be represented as

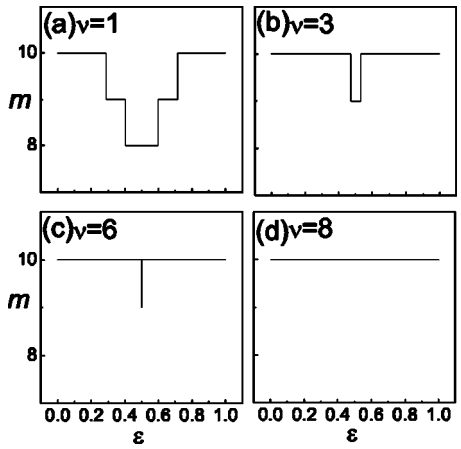

FIG. 3. The same as Fig. 1(b) by computing Eq. (6) for different ν's. We find $m \geqslant 8$ for $\nu \geqslant 1$. As ν is large ($\nu \geqslant 8$) the number of positive Lyapunov exponents saturates to the largest value $m=N=10$.

$$\lambda_1(\varepsilon,\nu) = \nu \ln 2 + \hat{\lambda}_1(\varepsilon). \tag{7}$$

In Fig. 2(f) we plot $\hat{\lambda}_1(\varepsilon)=\lambda_1(\varepsilon,\nu)-\nu \ln 2$ vs ε for different ν's ($\nu \geqslant 7$). It can be found that all data fall in an approximately identical curve, verifying the validity of Eq. (7).

In Fig. 3 we compute the Lyapunov exponent spectra of system (6) and plot the number of positive Lyapunov exponents m vs ε for different ν's. It is shown that we have $m \geqslant 8$ for $\nu \geqslant 1$ and $m=10$ for all $\nu \geqslant 8$. Therefore for large ν ($\nu \geqslant 8$) system (6) becomes strongly chaotic, and the chaotic attractor has the highest expansion dimension $m=10$ for the system size $N=10$. The scheme of Eq. (6) is surprisingly effective in increasing the expansion dimension.

For studying probability distributions of output sequences we do the same procedure as Fig. 1(c) in Figs. 4(a)–4(d) for different ν's. The distributions become more and more homogeneous as ν increases. One may measure the maximum and the minimum probability densities $\rho_{\max}(x_{\max})$ and $\rho_{\min}(x_{\min})$, and compute the largest deviation,

$$\Delta\rho = \rho_{\max}(x_{\max}) - \rho_{\min}(x_{\min}). \tag{8}$$

In Fig. 4(e) we plot $\Delta\rho$ vs ν for $\varepsilon=0.10$ (squares) and 0.30 (black dots), respectively. $\Delta\rho$ decreases quickly as ν increases. This behavior is expected since the linear amplification together with the modulo operation can effectively flatten the distribution. The behavior of Fig. 4(e) is observed for all different ε's tested in the regime $0<\varepsilon<1$. The controllability of the homogeneity of the probability distributions of the output chaotic sequences is greatly welcome when these systems are used as random number generators.

The last criterion of the chaoticity of Eq. (6) is its autocorrelations and mutual correlations. In Fig. 5 we plot the autocorrelations $C_{ii}(\tau)$ vs τ of Eq. (6) for different ε's and different ν's. It is observed that as ν becomes large (e.g., $\nu \geqslant 3$) we obtain $C_{ii}(\tau) \approx 0$ for $\tau \neq 0$. Exponential decays of

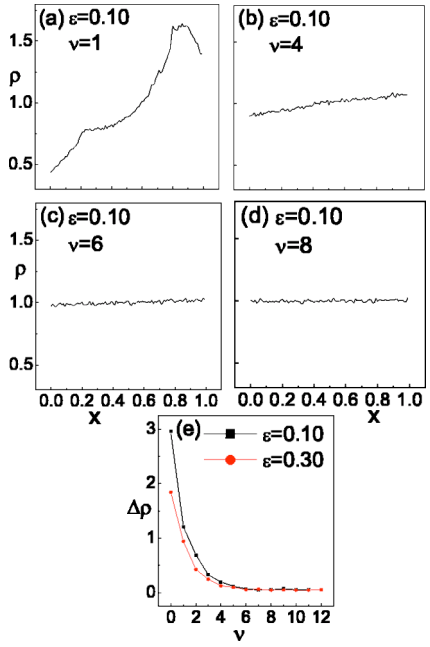

FIG. 4. (a)–(d) The same as Fig. 1(c) by computing Eq. (6) for different ν's. (e) $\Delta\rho$ defined in Eq. (8) plotted vs ν. As ν increases, $\Delta\rho$ goes to zero.

$C_{ii}(\tau)$'s with respect to ν are clearly shown in Fig. 5(d) for different τ's. In Figs. 6(a)–6(d) we plot the mutual correlations $C_{1i}(\tau)$'s, $i=2,3,4$ vs τ for different ε's and ν's. Again, exponential decays of $C_{1i}(\tau)$'s with respect to ν are justified. All results in Figs. 5 and 6 indicate that by increasing ν we can effectively decrease correlations of the output chaotic data for different times and different space units. The properties of small autocorrelation for $\tau\neq 0$, small mutual correlations, and effectiveness of the method in controlling these correlations are very crucial when chaoticity is required in practical applications.

In order to make a complete comparison of the dynamic features of Eq. (6) with those of Eq. (1), we do exactly the same in Figs. 7(a)–7(e) as in Figs. 1(a)–1(e) by replacing

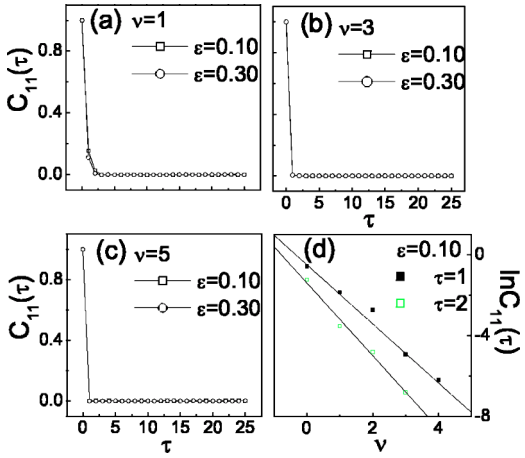

FIG. 5. The same as Fig. 1(d) by computing Eq. (6) for different ε's and ν's. As ν is large the autocorrelation goes to zero quickly as $\tau\neq 0$.

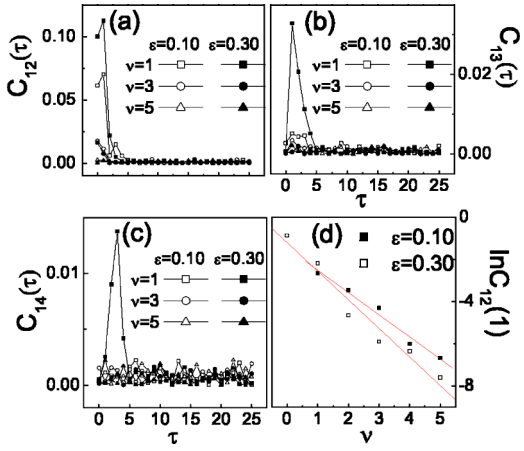

FIG. 6. (a)–(c) The same as Fig. 1(e) by computing Eq. (6) for different ν's. (d) $\ln C_{12}(\tau=1)$ plotted vs ν for different ε's.

Eq. (1) with Eq. (6) for $\nu=8$. It is remarkable that all the disadvantages of Fig. 1 mentioned in Sec. II are satisfactorily overcome in Fig. 7.

IV. EXTENSIONS AND DISCUSSIONS

In the last section we focused on a particular CML system Eq. (6) with the nonlinear function $f(x)=4x(1-x)$ and the system size $N=10$. The control mechanism of Eq. (6b) is generally effective for different coupled chaotic maps. For instance, we have studied in detail system (6) with $N=15$ and other larger sizes. The results are fully in agreement with those presented in Figs. 2–7. Moreover, the effectiveness of the above control method is independent of the form of the

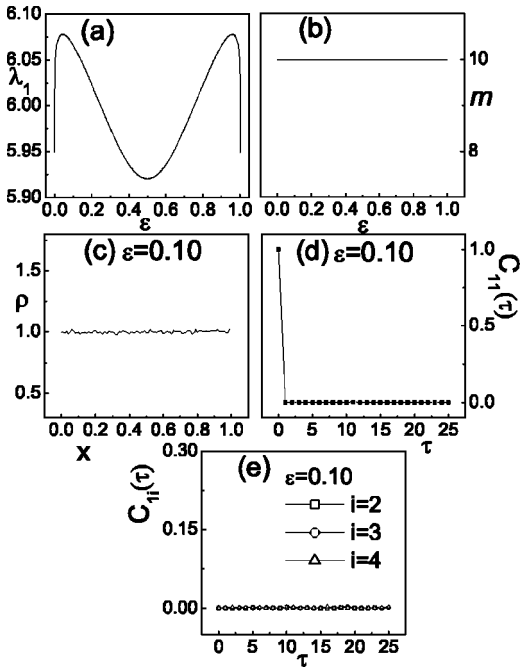

FIG. 7. (a)–(e) The same as Fig. 1(a)–1(e), respectively, with Eqs. (2) and (6) applied for computations. $\nu=8$. All the weak points of Eq. (1) manifested in Fig. 1 are satisfactorily overcome.

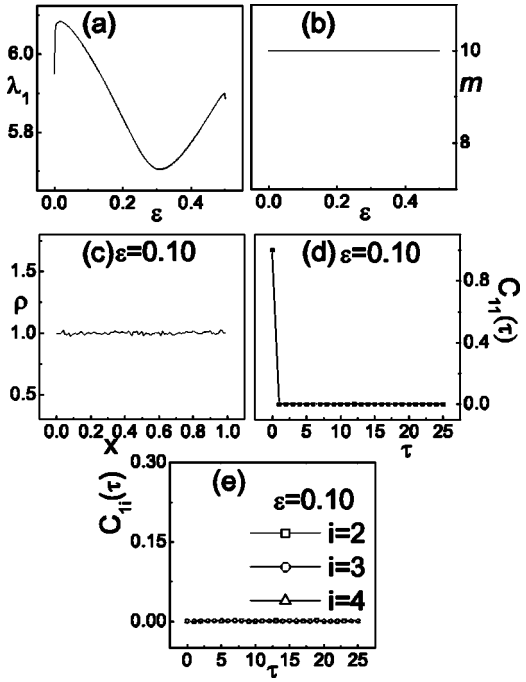

FIG. 8. (a)–(e) The same as Figs. 7(a)–7(e), respectively, with the symmetrical coupling Eq. (9) applied. All the behaviors of chaoticity of Fig. 7 are not changed by changing the coupling structure.

nonlinear function. We have used other nonlinear functions to replace the logistic function Eq. (2) [e.g., the tent map $f(x)=1-|2x-1|$, the sinusoidal map $f(x)=\sin(\pi x)$, and the exponential map $f(x)=x\exp(1-x_n)$] and got similar results. The effectiveness of this control scheme is also independent of the coupling structure. In Fig. 8, we use the following symmetrically coupled map lattice:

$$\hat{x}_{n+1}(i) = (1-2\varepsilon)f(x_n(i)) + \varepsilon[f(x_n(i-1)) + f(x_n(i+1))], \tag{9}$$

$$x_n(i) = [2^{\nu}\hat{x}_n(i)] \bmod 1, \quad f(x) = 4x(1-x),$$

and do exactly the same as in Fig. 7. Similar results can be obtained.

The method suggested in this paper is applicable not only to coupled chaotic maps, but also to other spatiotemporal systems, in particular to coupled chaotic oscillators with continuous time. Let us consider N coupled Rossler oscillators:

$$\dot{x}_i = -y_i - z_i + \varepsilon(x_{i+1} + x_{i-1} - 2x_i),$$

$$\dot{y}_i = x_i + ay_i + \varepsilon(y_{i+1} + y_{i-1} - 2y_i),$$

$$\dot{z}_i = b + (x_i - c)z_i + \varepsilon(z_{i+1} + z_{i-1} - 2z_i),$$

$$x_{i+N} = x_i, y_{i+N} = y_i, z_{i+N} = z_i, i = 1,2,\ldots,N. \tag{10}$$

When $a=0.45$, $b=2.0$, and $c=4.0$, the single Rossler oscillator is chaotic. In Fig. 9(a) we calculate the largest Lyapunov exponent λ_1 of the coupled system (10) against ε for $N=10$. It is obvious that nonchaotic windows corresponding to $\lambda_1=0$ exist in some ε regions. In Fig. 9(b) the number of positive Lyapunov exponents of Eq. (10) m is plotted against ε. m is small in a large ε region. Figures 9(a) and 9(b) show that the chaoticity of system (10) is weak in a large ε domain with small λ_1 and m. Now we modify Eq. (10) by kicked control, namely, by periodically resetting the variables by amplifications and modulo operations as

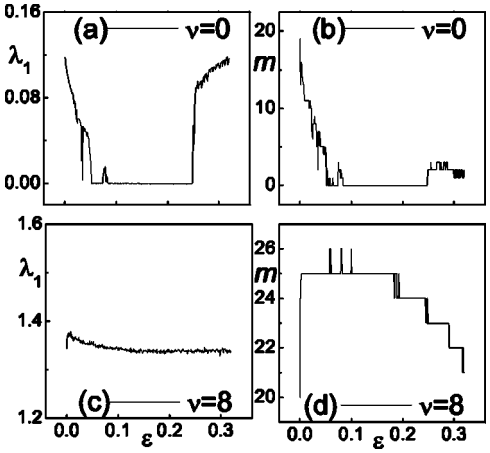

FIG. 9. $a=0.45$, $b=2.0$, $c=4.0$, and $N=10$ for Eq. (10). (a) The largest Lyapunov exponent λ_1 of Eq. (10) plotted vs ε. (b) The number of positive Lyapunov exponents m of Eq. (10) plotted vs ε. (c) and (d) The same as (a) and (b), respectively, by including the transformations Eq. (11) with $T=6.07$, $\alpha_1=31$, $\alpha_2=29$, $\alpha_3=35$, and $\nu=8$.

$$x(t \to nT+0) = F_1(x(t \to nT-0)),$$

$$y(t \to nT+0) = F_2(y(t \to nT-0)), \tag{11a}$$

$$z(t \to nT+0) = F_3(z(t \to nT-0)),$$

$$F_1(x) = 2^{\nu}x \bmod \alpha_1,$$

$$F_2(y) = 2^{\nu}y \bmod \alpha_2,$$

$$F_3(z) = 2^{\nu}z \bmod \alpha_3,$$

$$n = 1,2,3,\ldots. \tag{11b}$$

For $t \neq nT$ the dynamics of Eq. (10) is not changed. T is chosen to be $T=6.07$, which is the average phase period of the single Rossler equation for the given parameters, $\alpha_1=31$, $\alpha_2=29$, and $\alpha_3=35$, which are chosen as $(x_{\max}-x_{\min})$, $(y_{\max}-y_{\min})$, and $(z_{\max}-z_{\min})$, respectively, with $(x_{\max},y_{\max},z_{\max})$ and $(x_{\min},y_{\min},z_{\min})$ being the maximum and minimun values of (x,y,z) of Eq. (10). In Figs. 9(c) and 9(d) we do the same as in (a) and (b), respectively, by incorporating the modifications of Eq. (11). Considerable improvement of chaoticity is obviously observed in (c) and (d).

In conclusion, we have suggested an effective and practically realizable method, linear amplifications together with modulo operations, for spatiotemporal chaos control. The control purpose is to enhance chaoticity rather than suppress

chaos. We have successfully eliminated nonchaotic windows, increased the values and numbers of positive Lyapunov exponents, made the probability distributions of the output chaotic sequences more homogeneous, and reduced the correlations of chaotic sequences for different times and different space units. Though some of the observations, shown in Figs. 2 and 4, are intuitively expected and not surprising, the efficiency of all these improvements are impressive both theoretically and conceptionally. In particular, the possibility of applications is apparently significant.

Let us finish this presentation by a brief discussion on the applications of this method in designing optimal random-number generators and secure chaos-based cryptosystems. Since chaotic sequences have advantages of nonperiodicity, sensitive dependence on initial conditions, and randomlike behavior, the topics of applying chaotic systems to construct random-number generators and to design devices of secure communications have attracted much attention in the recent two decades [24–27]. However, it has been found that most of the chaos-based random-number generators and secure communication schemes previously proposed fail to exhibit the expected random and secure properties. The key reason is that chaotic dynamics can be easily reconstructed from the publicly transmitted signal [28–33]. Let us use Eq. (1) as an example to explain this point. We fix parameters $\varepsilon=0.10$ and $N=2$ and use the chaotic sequence of the second map $x_n(2)$ as our output. In Fig. 10(a) we numerically plot $x_n(2)$ against the pair of data $(x_{n-1}(2),x_{n-2}(2))$, and find that the function is smooth and the dynamics of the original chaotic system is practically reconstructable. With the function surface of Fig. 10(a) we can well predict the future output $x_n(2)$ from two previous successive data $x_{n-1}(2)$ and $x_{n-2}(2)$. Thus the system has very weak security and randomness.

Now we can compare the results of the modified system (6) with Fig. 10(a). In Figs. 10(b)–10(e) we do exactly the same as in Fig. 10(a) by computing Eq. (6) instead of Eq. (1). As ν increases the smoothness of the function $x_n(x_{n-1},x_{n-2})$ is severely broken, and the output becomes more and more random. Consequently, the predictability from (x_{n-1},x_{n-2}) to x_n becomes more and more difficult. This improvement of randomness is greatly significant since the control method is very simple and the level of security (i.e., randomness) can be well adjusted and controlled by choosing different ν. Of course, the behavior shown in Figs. 10(d) and 10(e) is only a necessary but not sufficient condition for constructing optimal random number generators and secure communications.

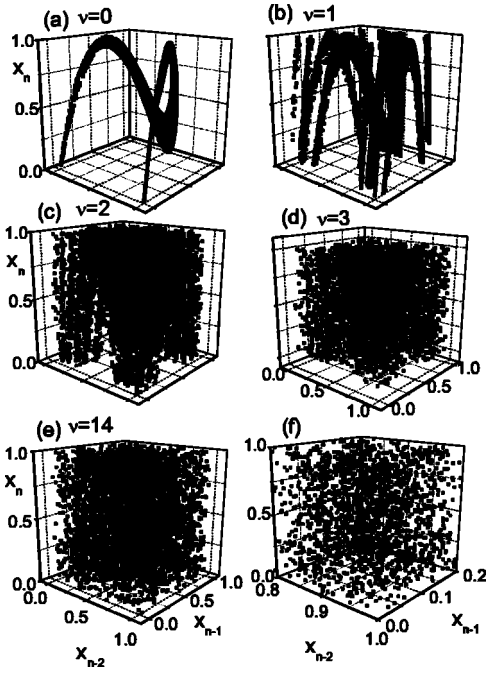

FIG. 10. Data plots in three-dimensional space $(x_n(2),x_{n-1}(2),x_{n-2}(2))$. $\varepsilon=0.1$, $N=2$, and arbitrary initial condition is adopted. $100\times100\times100$ mesh partition is applied and 10^4 data are used for the plots of each figure. (a) Equations (1) and (2) are applied, and continuous function relation of $x_n(2)$ to $(x_{n-1}(2),x_{n-2}(2))$ is observed. (b)–(e) The same as (a) with Eqs. (6) and (2) applied for $\nu=1,2,3,14$, respectively. (f) Blowup of a small region of (e).

ACKNOWLEDGMENTS

This work was supported by the National Natural Science Foundation of China (Grant Nos. 10335010, 70431002, and 10175010), and the Nonlinear Science Project. One of the authors (X.L.) was supported by the Special Funds for Excellent Doctoral Dissertations, the Huo-Ying-Dong Educational Funds for Excellent Young Teachers, and the Foundation for Doctoral Training.

[1] E. Ott, C. Grebogi, and J. A. Yorke, Phys. Rev. Lett. **64**, 1196 (1990).
[2] W. L. Ditto, S. N. Rauseo, and M. L. Spano, Phys. Rev. Lett. **65**, 3211 (1990).
[3] E. R. Hunt, Phys. Rev. Lett. **67**, 1953 (1991).
[4] R. Roy, T. Murphy, Jr., T. D. Maier, Z. Gills, and E. R. Hunt, Phys. Rev. Lett. **68**, 1259 (1992).
[5] U. Dressler and G. Nitsche, Phys. Rev. Lett. **68**, 1 (1992).
[6] V. Petrov, V. Gaspar, J. Masere, and K. Showalter, Nature (London) **361**, 240 (1993).
[7] P. Parmananda, P. Sherard, R. W. Rollins, and H. D. Dewald, Phys. Rev. E **47**, R3003 (1993).
[8] G. R. Chen and X. N. Dong, *From Chaos to Order* (World Scientific, Singapore, 1998).
[9] S. J. Schiff, K. Jerger, D. H. Duong, T. Chang, M. L. Spano, and W. L. Ditto, Nature (London) **370**, 615 (1994).
[10] W. Yang, M. Ding, A. Mandell, and E. Ott, Phys. Rev. E **51**, 102 (1995).
[11] Visarath In, Susan E. Mahan, William L. Ditto, and Mark L. Spano, Phys. Rev. Lett. **74**, 4420 (1995).

[12] N. Gupte and R. E. Amritkar, Phys. Rev. E **54**, 4580 (1996).
[13] Ira B. Schwartz and Ioana Triandaf, Phys. Rev. Lett. **77**, 4740 (1996).
[14] P. Parmananda and M. Eiswirth, Phys. Rev. E **54**, R1036 (1996).
[15] R. Ramaswamy, S. Sinha, and N. Gupte, Phys. Rev. E **57**, R2507 (1998).
[16] Soumitro Banerjee, James A. Yorke, and Celso Grebogi, Phys. Rev. Lett. **80**, 3049 (1998).
[17] X. F. Wang and G. R. Chen, Int. J. Bifurcation Chaos Appl. Sci. Eng. **10**, 549 (2000).
[18] G. Q. Zhong, K. F. Man, and G. Chen, Int. J. Bifurcation Chaos Appl. Sci. Eng. **11**, 865 (2002).
[19] K. Kaneko, Phys. Lett. **111A**, 397 (1985).
[20] R. J. Deissler, Phys. Lett. A **120**, 334 (1987).
[21] R. J. Deissler and K. Kaneko, Phys. Lett. A **119**, 397 (1987).
[22] R. J. Deissler, Physica D **25D**, 23 (1987).
[23] I. S. Aronson, A. V. Gaponov-Grekhov, and M. I. Rabinovich, Physica D **33D**, 1 (1988).
[24] L. M. Pecora and T. L. Carroll, Phys. Rev. Lett. **64**, 821 (1990).
[25] L. Kocarev, K. S. Halle, K. Eckert, L. O. Chua, and U. Parlitz, Int. J. Bifurcation Chaos Appl. Sci. Eng. **2**, 709 (1992).
[26] K. M. Cuomo and A. V. Oppenheim, Phys. Rev. Lett. **71**, 65 (1993).
[27] D. G. Van Wiggeren and R. Roy, Science **279**, 1198 (1998).
[28] K. M. Short, Int. J. Bifurcation Chaos Appl. Sci. Eng. **4**, 959 (1994).
[29] G. Perez and H. Cerdeira, Phys. Rev. Lett. **74**, 1970 (1995).
[30] K. M. Short and A. T. Parker, Phys. Rev. E **58**, 1159 (1998).
[31] Ch. S. Zhou and C. H. Lai, Phys. Rev. E **60**, 320 (1999).
[32] Ch. S. Zhou and C. H. Lai, Phys. Rev. E **59**, 6629 (1999).
[33] V. I. Ponomarenko and M. D. Prokhorov, Phys. Rev. E **66**, 026215 (2002).